Conformational Analysis. 24. Structure and Composition of Gaseous Oxalyl Fluoride, $C_2F_2O_2$: Electron-Diffraction Investigation Augmented by Data from Microwave Spectroscopy and Molecular Orbital Calculations

Dwayne T. Friesen,[†] Tom R. Borgers,[‡] Lise Hedberg, and Kenneth Hedberg*

Department of Chemistry, Oregon State University, Corvallis, Oregon 97331-4003

Received: April 26, 2006; In Final Form: August 24, 2006

The molecular structure and composition of gaseous oxalyl fluoride (OXF) has been investigated by electron diffraction (GED) at nozzle-tip temperatures of −10, 149, and 219 °C. The GED data were augmented by molecular orbital calculations, and the analysis was aided by use of rotational constants from microwave (MW) spectroscopy. As in the other oxalyl halides, there are two stable species, of which the more stable is periplanar anti (i.e., trans). However, unlike these other halides in which the second form is gauche, the second form of oxalyl fluoride was known from MW work to be periplanar syn (i.e., cis). Our results are consistent with a mixture of trans and cis forms, and yield values for the structural parameters, the composition of the system at the three temperatures cited, and the thermodynamic quantities $\Delta G°$, $\Delta H°$, and $\Delta S°$ for the reaction trans → cis. Some trans/cis distances (r_g/Å) and angles ($\angle_\alpha$/deg) at −10 °C are r(C═O) = 1.178(2)/1.176(2), r(C−F) = 1.323(2)/1.328(2); r(C−C) = 1.533(3)/1.535(3), ∠(C−C═O) = 126.4(2)/124.2(2), ∠(C−C−F) = 109.8(2)/112.2(2), and ∠(O−C−F) = 123.8(2)/123.6(2). The mixture compositions (percent trans) at −10 °C/149 °C/219 °C are 75(3)/58(7)/52(8), from which $\Delta H°$ and $\Delta S°$ are found to be 1.14 kcal/mol and 2.12 cal/(mol·deg). The system properties are discussed.

Introduction

Investigation of the structures and compositions of the oxalyl halides (XOC−COY, Figure 1) has a long history. It was known over four decades ago that the molecules of oxalyl chloride (OXCL) and oxalyl bromide (OXBR) have a centrosymmetric trans[1] form in the crystal.[2] Some analyses of the IR and Raman spectra of OXCL[3] and OXBR,[4,5] and their homologues oxalyl fluoride (OXF)[6] and oxalyl chloride fluoride (OXCLF), led to the conclusion that this form was likely the only one present in the liquid and gas phases as well. However, other IR and Raman studies of these substances (OXCL,[7] OXBR,[8] OXF,[9,10] OXCLF) suggested that, in addition to the expected planar trans form, a second conformer, universally assumed to be the planar cis form of C_{2v} symmetry, was also present in the fluid phases.

The uncertainties about the nature, even the existence, of a second form of these molecules impelled us to undertake electron-diffraction (GED) investigations of their vapors. The first of these investigations, on OXCL, indicated that a second conformer did indeed exist, but rather unexpectedly it was not cis, but a gauche form with a torsion angle of about 55° from the planar cis.[11] Subsequent molecular orbital calculations[12] at several levels of theory and basis-set size again raised the question about the existence of a second form because only one distinct minimum in the potential (at the trans angle) was found. However, the shape of the potential was very sensitive to the type of calculation, and in many cases was quite flat over a (gauche) range centered at 90° where the calculated energy was only a fraction of a kilocalorie per mole higher than that of the trans form. To clarify the situation, the GED data were reanalyzed in terms of a more elaborate model. In the early work,[10] where the results of molecular orbital theory were not readily available, the system model consisted of an assumed trans molecule and a second form that differed structurally only in its torsion angle. With molecular orbital (MO) results now easily obtainable, the indicated changes in structure that occurred with changes in torsion angle could be incorporated into the model. The results of a new analysis[13] based on such a model using the GED data augmented by additional MO calculations provided a more complete picture of the system than the earlier study. As before, gaseous OXCL was found to consist of the more stable trans form and a second gauche form, with the latter having its potential minimum at a somewhat smaller Cl−C−C−Cl torsion angle of 89.8°. However, this potential minimum is shallow with a very small gauche → trans barrier of about 0.1 kcal/mol. (The implications of this circumstance will be discussed later.) OXBR was investigated[14] by GED a short time after the original OXCL work, and later OXCLF was also studied.[15] The second form in each of these systems was found to be gauche instead of the postulated cis.[8,9] The subsequent developments in the OXCL models suggests that these systems should also be be reexamined, but that has not yet been done.

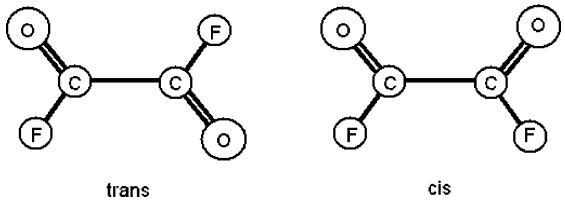

Figure 1. Diagrams of the trans and cis forms of oxalyl fluoride.

The structural history of OXF is similar to that of OXCL. As cited above, the early spectroscopic work pointed to the

* To whom correspondence should be addressed. E-mail:ken.hedberg@oregonstate.edu.

[†] Present address: Bend Research, Inc., 64550 Research Road, Bend, OR 97701.

[‡] Present address: P.O. Box 66, Bayside, CA 95524.

10.1021/jp062575+ CCC: $33.50
Published on Web 11/10/2006

presence of only one species of the molecule in both liquid and gas (trans), but the later work indicated the presence of a second form which was again assumed to be cis. Our GED investigation of the structure and composition of the OXF system has been an "off and on" experience that began four decades ago and was completed up to the standards of the time by Friesen in 1981. However, the results were not published. The reasons for the delay are several, but the most important was our uncertainty about the identity of the second conformer, even though interpretations of the diffraction data seemed to favor it as cis. This uncertainty was recently removed by microwave (MW) spectroscopic work[16] which proved this form to indeed be the cis, and yielded a form for the rotational potential and the thermodynamic functions $\Delta G°$ and $\Delta S°$ at −78 °C. With the question of the identity of the second conformer now unequivocally answered, it seemed time to revisit the still-remaining questions about the OXF system. These questions were the values of the structural parameters of the molecules, the system composition and its variation with temperature, and the values of thermodynamic functions $\Delta G°(T)$, $\Delta E°$, and $\Delta S°$, all of which could be addressed with our previous diffraction data that had been gathered at several temperatures. Although answers to these questions were obtained from the previous work, we expected the reanalysis of these data to yield more reliable results through the use of more elaborate models now made possible by advances in the feasibility of theoretical calculations.

Experimental Section

Over the lengthy course of this investigation several samples of OXF have been used, most of which were of uncertain purity. The sample on which the present report is based was obtained in 1980 from Columbia Organic Chemicals. It was purified by a series of trap-to-trap distillations. From the appearance of the IR spectrum, the final product was estimated to be about 99% pure. Diffraction experiments were done with the OSU apparatus under the following conditions: sector shape, r^3; photographic plates, 8 × 10 in Kodak Lantern Slide medium contrast, developed in D19 diluted 1:1 for 10 min; exposure times, 80−170 s; beam currents, 0.38−0.48 μA; (nominal) electron wavelengths, 0.056−0.058 Å calibrated against patterns of CO_2 obtained from separate experiments taking $r_a(CO) = 1.1646$ Å and $r_a(OO) = 2.3244$ Å; ambient apparatus pressure during sample run-in, 8.2×10^{-6} Torr. Experiments were carried out at nozzle-tip temperatures of −10, 149, 219, and 321 °C. Preliminary work revealed that decomposition had occurred at the two higher temperatures. The amount was slight at 219 °C, but too great at 321 °C to permit a reliable determination of the properties of interest. We therefore discarded the 321 °C data and limited our analyses to the data from the three lower temperatures. Four plates made at each camera distance for the two lowest temperatures, and four plates from the long and two from the intermediate camera distance for the 219 °C experiment, were selected for the structure analysis.

Reduction of the diffraction data and the preparation of the scattered molecular intensities were done by methods previously described.[17] Radial distribution curves were calculated from composites of the molecular intensities after multiplication of them by $Z_C Z_F/(A_C A_F) \exp(-0.002s^2)$, where $A = s^2F$. The electron-scattering amplitudes and associated phases were obtained from tables.[18] Curves of the intensities from the −10 °C data are shown in Figure 2; curves from the other temperatures are similar. The radial distribution curves for the systems at the three temperatures of interest are shown in Figure 3. The

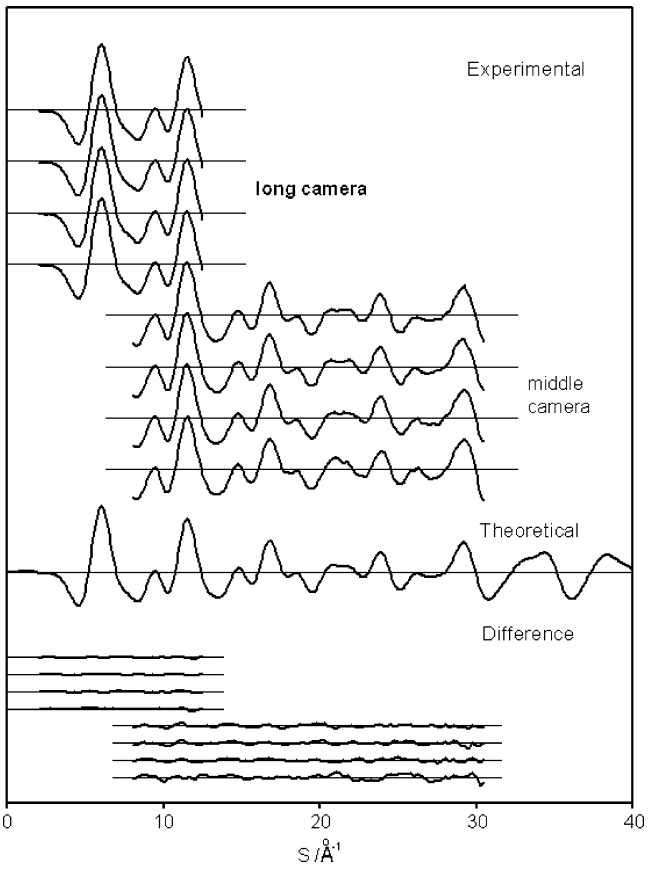

Figure 2. Molecular intensity curves for the experiment at −10 °C. The theoretical curve is from the final model. Difference curves are experimental minus theoretical.

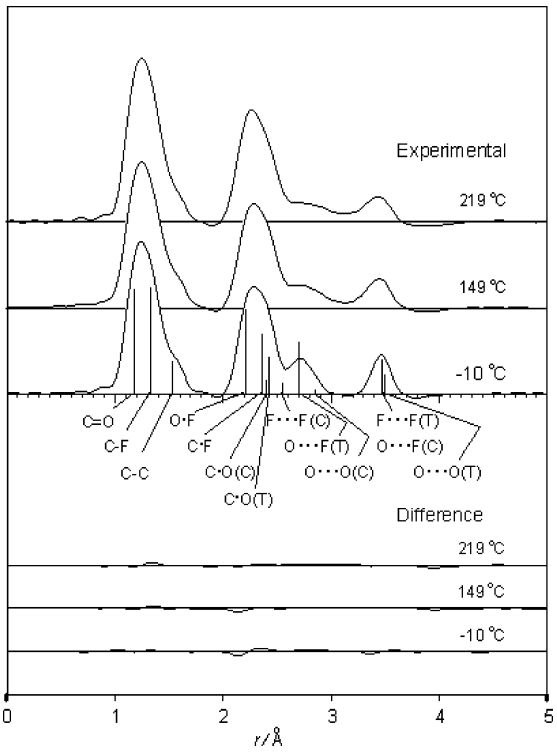

Figure 3. Radial distribution curves. The vertical lines mark the positions of interatomic distances; their lengths are proportional to the scattering power of the term at −10 °C. Difference curves are experimental minus theoretical.

TABLE 1: Theoretical Energies of the trans and cis Forms of Oxalyl Fluoride

	trans		cis		cis−trans[a]
theory/basis	E_h + 424.0	ZPE	E_h + 424.0	ZPE	ΔE/kcal·mol^{-1}
HF/6-31G(d)	−0.335 458 4	0.026 241 7	−0.333 944 5	0.026 138	0.885
B3LYP/6-311+G(d)	−2.469 503 9	0.023 081 0	−2.468 712 8	0.022 980	0.433
B3LYP/aug-cc-pvtz	−2.508 504 8	0.023 108	−2.507 560 2	0.022 986	0.516
MP2/aug-cc-pvtz	−1.782 284 6	0.023 101	−1.781 263 5	0.022 965	0.555

[a] Energy difference taking zero point energies into account.

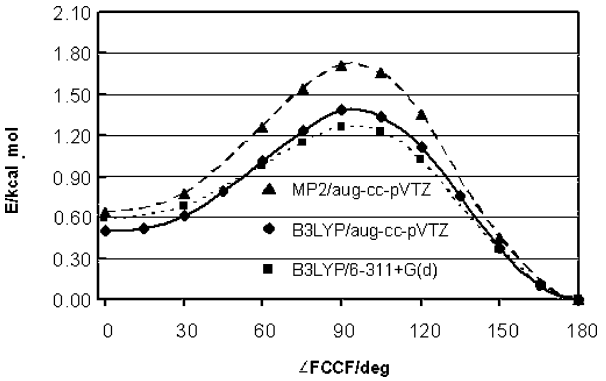

Figure 4. Theoretical energies of conformations as a function of torsion angle.

numerical molecular intensity data for the three lowest temperatures are available as Supporting Information.

Structure Analysis

Theoretical Calculations. The complexity of the OXF system required results from molecular orbital and normal-coordinate calculations for all aspects of the structure analysis. We carried out the MO calculations with the Gaussian 98 and 03[19] program packages at the HF, B3LYP, and MP2 levels of theory with various basis sets, principally 6-31G(d), 6-311+G(d), and aug-cc-pVTZ. The energies for the optimized cis and trans forms obtained from some of these are given in Table 1. We also mapped the torsional potential for OXF by optimizing structures with three of these theory/basis-set combinations over the full 180° range of the torsion angle F−C−C−F: B3LYP/6-311+G(d) at 15° intervals, and B3LYP/aug-cc-pVTZ and MP2/aug-cc-pVTZ at 0°, 30°, 60°, 75°, 90°, 105°, 120°, 150°, and 180°. Figure 4 shows curves of the results.

Harmonic frequency calculations were carried out for the cis and trans conformers with theory/basis-set combinations listed in Table 1. Using the symmetrized Cartesian force field from the B3LYP/6-311+G(d) frequency calculation, normal-coordinate calculations were then carried out with the program ASYM40[20] in order to obtain values for the various corrections used in the interconversion of distance types, and for amplitudes of vibration that could provide information about those that were unaccessible experimentally. Table S1 in the Supporting Information shows the symmetry coordinates and symmetry force field, Table S2 identifies the internal coordinates used to make up the symmetry coordinates, and Table S3 contains a list of the experimental and theoretical wavenumbers of the two forms together with a description of the modes.

Models. Given that the system consists of a pair of cis and trans conformers subject to large amplitude torsional motion, three models suggest themselves. One of these consists of just these two forms defined by ∠(F−C−C−F) equal to 0° and 180°, each form undergoing small amplitude harmonic vibration. A second model is a slightly more sophisticated version of the two-conformer model and should be better in the event that the

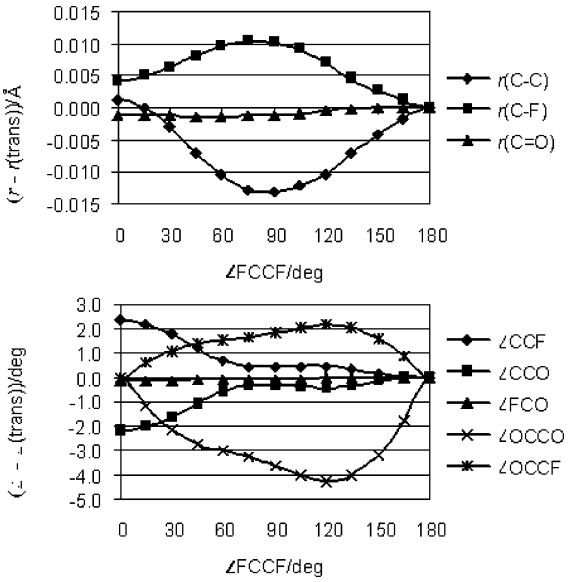

Figure 5. Theoretical (B3LYP/6-311+G(d) variation of bond distances and bond angles with torsion angle.

torsional motions of each conformer are of large amplitude. This model depicts the torsion of each form in terms of a set of pseudoconformers, each pseudoconformer characterized by a different torsion angle close to 0° or 180°, and is given a Boltzmann weight that reflects its contribution to the shape of the distribution of the torsion-sensitive distances. The third model consists of a set of pseudoconformers, not localized around the cis and trans torsion angles, but positioned at a constant interval over the full torsion-angle range of 0°−180°; this model would be most appropriate for a system with a low torsional barrier and thus very large torsional motions centered at the planar trans and cis torsion angles. For several reasons it appeared that the torsional amplitudes had to be very large, and this together with other considerations led us to base our analysis on the last type of model.[21] Such a model is in principle a collection of OXF molecules each differing from the others not only in the torsion angle, but also in their bond lengths and bond angles and in the vibrational amplitudes of the molecular frames. These parameters cannot be separately measured; instead some relationship among them must be invoked to make the problem tractable. For this purpose we used the bond-length, bond-angle, and amplitude *differences* obtained from theory (B3LYP/6-311+G(d)), i.e., structure optimizations carried out for each member of the set of pseudoconformers. The bond-length and bond-angle differences are seen in Figure 5. With the assumption of these differences, the entire system can be defined in terms of the structural and vibrational amplitude parameters of one pseudoconformer and the parameters of the potential function chosen to describe the torsion.

We chose the structural parameters of the planar trans form of OXF as the basis for the refinements. The pseudoconformers were 25 in number, covering the range 0°−180° at intervals of 7.5°. The torsional potential was assumed to have the form

$$V = (1/2)[V_1(1 - \cos\phi) + V_2(1 - \cos 2\phi) + V_3(1 - \cos 3\phi)] \quad (1)$$

where $\phi = 0$ corresponds to the trans conformation,[22] and each pseudoconformer was given the weight $Q^{-1} \exp[-V(\phi_i)/RT]$ with $Q = \sum_i \exp[-V(\phi_i)/RT]$. Specification of the system was done in $r_\alpha^0 = r_z$ space because we wished to make use of the rotational constants for the cis form available from the MW work. The structure-defining parameters for the planar trans form were the bond lengths r_α^0(C−C), r_α^0(C−F), and r_α^0(C═O) and the bond angles $\angle_\alpha$(C−C═O) and $\angle_\alpha$(C−C−F). The structure of each pseudoconformer was generated from the parameter differences described above. The vibrational parameters were the amplitude groups *l*(C═O,C−F,C−C), *l*(O·F,C·F,C·O), and *l*(O··F,C··F,C··O); the differences between members of the amplitude groups were obtained from the ASYM40 calculations based on the quadratic force field from the B3LYP/6-311+G-(d) calculation. The three potential constants in eq 1 were also refined. They provide a basis for the determination of the cis−trans composition of the system.

The refinements of system properties for each of the three experimental temperatures were done by least squares, simultaneously fitting theoretical diffraction data and the rotational constants for the s-cis form to the corresponding experimental quantities. Instead of averages of the experimental diffraction data from each camera distance, we used the individual sets, i.e., one from each plate. The three rotational constants in megahertz ($A_0 = 5902.909$, $B_0 = 3588.582$, and $C_0 = 2240.758$) were converted to B_z ($A_z = 5941.269$, $B_z = 3598.132$, and $C_z = 2240.318$) and given weights that led to a weighted sum of squares of residuals about 20 times smaller than those from the diffraction data. Under these conditions the refinements proceeded smoothly to convergence, giving the results summarized in Table 2. (To obtain the composition, it was necessary to examine the distribution of the pseudoconformers determined by the three torsional potential constants. This and other matters are taken up in the following section.) The quality of the fits is good, as may be judged from the difference curves in Figures 2 and 3, the values of the *R*-factors in Table 2, and the rotational constant differences (observed minus calculated) which are, respectively, at −10, 149, and 219 °C equal to 4.883, 2.456, and 0.895 MHz for ΔA_z; 1.446, 0.281, and 0.232 MHz for ΔB_z; and 0.608, −0.189, and −0.430 MHz for ΔC_z.

Discussion

Structure. The important features of the system concern the structures of the trans and cis forms of the molecules, each of which has planar C_2FO groups. Although the structures of the nonplanar pseudoconformers are not experimentally accessible, theory indicates that the C_2FO groups deviate significantly from planarity: Figure 5 shows the O═C−C═O angle to be about 4° less than the F−C−C−F angle at values of F−C−C−F near 120°.

The data of Table 2 show that the bond distances in the two forms of OXF differ very little and are unaffected by change in temperature. Also, the effect of temperature on the bond angles is seen to be negligible. However, there are appreciable differences between the trans minus cis values of the C−C−F and C−C═O angles, which are such as to leave the O═C−F angle with the same value (123.7(2)°) in the two forms. Thus, although the trans minus cis values for the F−C═O angle are 0.2° or less at each temperature, the C−C═O and C−C−F values are respectively about 2.2° greater and 2.3° less in the trans than in the cis form. These data correspond to a rocking of the O═C−F groups that brings the oxygen atom closer to the geminal carbon atom in the cis form than in the trans. The rocking is doubtless a response to steric repulsion: without the rock the O···O distance would be about 2.94 Å and the F···F about 2.45 Å; with it these become 2.86 and 2.54 Å. The motivating interaction is likely the F···F distance, for which the van der Waals contact is about 2.7 Å (the O···O van der Waals distance is about 2.8 Å).

There are interesting similarities and differences between the structures of OXF and acetyl fluoride. According to a combined GED + MW[23] study of acetyl fluoride, the C═O bond length (1.185(2) Å) is almost identical to that in OXF, the C−F (1.362-(2) Å) is 0.03 Å longer, and the C−C (1.505(21) Å) is 0.03 Å shorter; the O═C−F, C−C−F, and C−C═O bond angles are respectively 3° smaller, 1° smaller, and 2° larger than in OXF. (Comparison values used for OXF are averages of trans and cis.) One may account for these differences in terms of bonding effects as follows. The −CO(F) groups in OXF are each strongly electron-withdrawing, which leads to a smaller bond order between the two carbon atoms and hence to a longer C−C bond than in acetyl fluoride. The corresponding increase in the bonding power within the −CO(F) groups is channeled into the C−F bonds, which increases their double-bond character, thus shortening them. At the same time the augmented C−F double-bond character, the lower bond order of the C−C bond, and the existing C═O (double) bond combine to suggest rehybridization of the σ-bonds within the −CO(F) groups in the direction of more sp character, which leads to an increased O═C−F bond angle. These bonding effects should be largely absent in acetyl fluoride, and it is therefore surprising that the geminal distances of the same type in the two molecules have nearly the same value: in OXF/acetyl fluoride in angstroms, 2.41/2.43 for C·O, 2.36/2.36 for C·F, and 2.21/2.21 for O·F. Such geminal-distance similarities argue strongly for the importance of nonbond repulsion in determining the shapes of the C−CO(F) groups in both molecules.

A question of great interest is the planarity of the cis form of OXF in view of the nonplanar gauche form of the less stable conformers in the other oxalyl halides. The reason is likely a combination of the opposing effects of bond conjugation tending to stabilize a planar form and steric repulsion tending to destabilize it. Bond conjugation should be greater in OXF than in the other halides due to the greater ability of the fluorine atoms to engage in back π-bonding and thus to confer partial double bond character to the C−F bonds represented by the valence-bond structure $^-C{=}F^+$. On the other hand, van der Waals (vdW) steric repulsion between the halogen atoms should be less in OXF than in the other halides. For example, if one assumes the distance difference *cis*-X···X(exptl) minus *cis*-X···X(vdW) to be a measure of the repulsion, greater repulsion is indicated by greater negative values. This difference is only −0.2 Å in OXF, but for a *cis*-Cl···Cl distance in OXCL it would be −0.5 Å.

A similar situation exists for the gaseous molecules of diboron tetrafluoride ($F_2B{-}BF_2$),[24] which is planar, and diboron tetrachloride ($Cl_2B{-}BCl_2$),[25] which is staggered. Again, back π-bonding of the type $^-B{=}X^+$ is expected to be more important for the fluoride than for the chloride, and steric repulsion for a planar diboron tetrachloride would be slightly greater than that for the fluoride. Concerning these steric effects, in the choride (were it to be planar) the vdW distance for *cis*-X···X is greater than the predicted experimental one by about 0.1 Å, indicative of slight repulsion, but in the fluoride the vdW distance is about 0.4 Å less than the measured value. Similar arguments apply

TABLE 2: Structural Parameter Values for Oxalyl Fluoride[a]

	−10°					149°					219°				
parameter	r_α^0; $\angle_\alpha$	r_g; $\angle_g$	r_a; $\angle_a$	l		r_α^0; $\angle_\alpha$	r_g; $\angle_g$	r_a; $\angle_a$	l		r_α^0; $\angle_\alpha$	r_g; $\angle_g$	r_a; $\angle_a$	l	
trans Form															
r(C═O)	1.178(2)	1.181	1.179	0.039		1.176(2)	1.180	1.178	0.052		1.178(2)	1.183	1.181	0.046	
r(C−F)	1.323(2)	1.327	1.325	0.049	(3)	1.323(2)	1.327	1.324	0.063	(3)	1.324(2)	1.329	1.327	0.057	(3)
r(C−C)	1.533(3)	1.536	1.534	0.055		1.539(3)	1.542	1.539	0.070		1.535(3)	1.538	1.535	0.065	
∠(C−C═O)	126.4(2)	126.1	126.2			126.6(3)	126.3	126.5			127.2(3)	126.8	126.9		
∠(C−C−F)	109.8(2)	109.7	109.7			109.4(3)	109.2	109.3			109.1(3)	109.6	109.0		
r(O·F)	2.207(2)	2.209	2.208	0.052		2.207(2)	2.210	2.208	0.064		2.208(2)	2.211	2.209	0.067	
r(C·F)	2.341(3)	2.343	2.341	0.065	(3)	2.339(4)	2.342	2.339	0.081	(3)	2.333(4)	2.336	2.333	0.085	(4)
r(C·O)	2.425(3)	2.427	2.425	0.061		2.431(4)	2.434	2.431	0.075		2.435(5)	2.438	2.435	0.079	
r(O···F)	2.698(3)	2.699	2.696	0.091		2.697(3)	2.699	2.694	0.119		2.699(3)	2.701	2.694	0.136	
r(O···O)	3.490(5)	3.491	3.491	0.054	(5)	3.495(6)	3.497	3.496	0.070	(7)	3.504(7)	3.505	3.504	0.082	(10)
r(F···F)	3.480(4)	3.481	3.480	0.058		3.474(5)	3.476	3.474	0.076		3.469(6)	3.471	3.469	0.088	
cis Form															
r(C═O)	1.176(2)	1.180	1.178	0.039		1.175(2)	1.179	1.176	0.052		1.177(2)	1.181	1.180	0.046	
r(C−F)	1.328(2)	1.331	1.329	0.049	(3)	1.327(2)	1.331	1.328	0.063	(3)	1.328(2)	1.333	1.331	0.058	(3)
r(C−C)	1.535(3)	1.537	1.535	0.055		1.540(3)	1.543	1.540	0.070		1.536(3)	1.539	1.536	0.065	
∠(C−C═O)	124.2(2)	123.9	124.0			124.4(3)	124.1	124.3			124.9(3)	124.6	124.7		
∠(C−C−F)	112.2(2)	112.0	112.1			111.7(3)	111.5	111.7			111.5(3)	111.2	111.4		
r(O·F)	2.208(2)	2.210	2.209	0.053		2.208(2)	2.211	2.209	0.065		2.209(2)	2.212	2.210	0.068	
r(C·F)	2.378(3)	2.380	2.379	0.064	(3)	2.376(4)	2.379	2.376	0.080	(3)	2.370(4)	2.374	2.371	0.085	(5)
r(C·O)	2.401(3)	2.403	2.402	0.062		2.407(4)	2.410	2.408	0.076		2.411(5)	2.414	2.412	0.080	
r(O···F)	3.482(3)	3.483	3.482	0.056		3.480(4)	3.482	3.480	0.074		3.481(4)	3.482	3.480	0.086	
r(O···O)	2.856(7)	2.857	2.854	0.086	(5)	2.868(10)	2.869	2.864	0.112	(7)	2.884(12)	2.885	2.879	0.128	(10)
r(F···F)	2.537(7)	2.539	2.536	0.092		2.523(10)	2.526	2.520	0.122		2.509(12)	2.512	2.504	0.139	
V_1	0.48(17)					0.44(25)					0.23(32)				
V_2	1.39(16)					1.12(17)					1.06(22)				
V_3	0.64(21)					0.42(32)					0.38(46)				
% s-trans	75(3)					58(7)					52(8)				
% decomp[b]	[0]					[0]					[12]				
R[c]	0.80					0.86					0.77				

[a] Distances (*r*) and amplitudes (*l*) in angstroms, angles (−) in degrees. Quantities in parentheses are estimated 2σ. Uncertainies for r_g, $-_g$, r_a, and $-_a$ are assumed to be the same as for r_α and $-_\alpha$. [b] Tested but not refined. [c] $R = [\sum_i w_i \Delta_i^2 / \sum_i w_i (s_i I_{m,i}(\text{obsd}))^2]^{1/2}$, where $\Delta_i = s_i I_{m,i}(\text{obsd}) - s_i I_{m,i}(\text{calcd})$.

to diboron tetrabromide (staggered). They also apply to a different type of molecule, dinitrogen tetroxide (O_2N-NO_2). This molecule is planar in the gas, apparently more rigidly so than F_2B-BF_2, despite having an extraordinarily long N−N bond[26] that corresponds to only about 0.3 of a normal single bond. In O_2N-NO_2 the experimental distance between the *cis*-oxygen atoms is 2.69 Å and the vdW distance is 2.8 Å, implying that a small amount of repulsion should exist. Even so, despite the long N−N bond the conjugation energy seems to be sufficient to maintain both the planarity of the molecule and a larger barrier to internal rotation than in F_2B-BF_2. This circumstance doubtless arises from a π-electron density that is naturally resident on the nitrogen atoms and is higher than that obtained from the back π-bonding cited for the B−F bonds in F_2B-BF_2. Finally, one is struck by the fact that the molecules diboron tetrafluoride and OXF have homologues to which they are chemically similar but conformationally different, yet which, together with dinitrogen tetroxide, comprise a group of molecules that are conformationally similar but have very different chemistries. One property these molecules have in common is their isoelectronicity: it is surely this property that is responsible for the similarity in the shapes of their conformers.

Isomeric Composition and Thermodynamic Quantities. To describe the system in terms of a mixture of cis and trans conformers requires that the set of pseudoconformers comprising our model be divided into two groups centered at ∠(F−C−C−F) equal to 0° and 180°. Our structure refinements yielded values of the three potential constants in eq 1 from which the distribution of the pseudoconformers could be calculated. Plots of the distributions at the three temperatures of interest are shown in Figure 6. We took the dividing line to be at the minima in the distribution of pseudoconformers, i.e., at ∠(F−C−C−F) equal to 100°,[27] and determined the areas under each curve on either side of this line. With the total normalized to unity, the ratio of these areas gives the cis−trans composition at the indicated temperature. The results are given in Table 2.

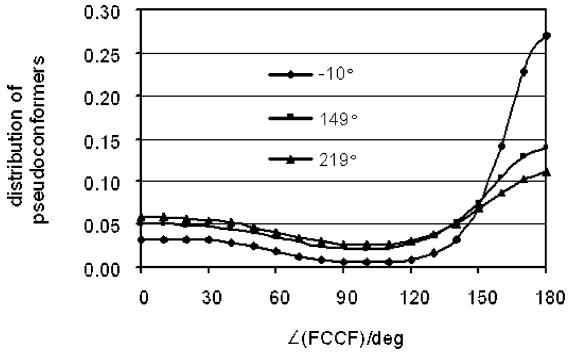

Figure 6. Experimental distribution of conformations from experiments at different temperatures.

The variation of the compositions (i.e., the equilibrium constants for the trans to cis reaction) with temperature affords the opportunity to estimate the enthalpy and entropy of the reaction from the usual formula $\Delta G° = -RT \ln K$. Figure 7 is a van't Hoff plot, the slope of which yields $\Delta H°_{exp} = 1.14$ kcal/mol and the intercept yields $\Delta S°_{exp} = 2.12$ cal/(mol·deg). It is not clear how to draw a useful comparison between these values and those from theory. For example, the energy difference ($\Delta E°$) is obtained by theory at 0 K only for molecules defined by torsion angles of 0° and 180°, whereas our GED results are derived from molecules over all torsion angles, reflect thermal averaging, and yield $\Delta G°$ directly. If one applies the predicted (harmonic) temperature-dependent corrections to the theoretical

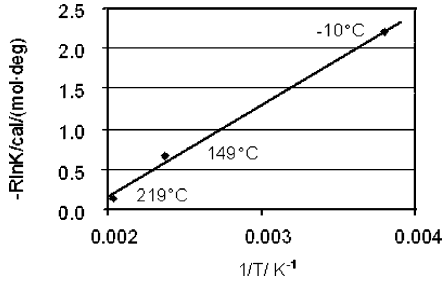

Figure 7. van't Hoff plot for determination of experimental values of thermodynamic quantities. K = [cis]/[trans].

(B3LYP/6-311+G(d)) $E°$ values for the cis and trans conformers, one obtains the values $\Delta H°_{theor} = 0.45$ kcal/mol and $\Delta S°_{theor} = 0.9$ cal/(mol·deg), which are significantly smaller than the experimental ones. The values of $\Delta H°_{theor}$ from other levels of theory are quite similar, but those for $\Delta S°_{theor}$ increase: 1.5 cal/(mol·deg) from B3LYP/aug-cc-pvtZ and 2.3 cal/(mol·deg) from MP2/aug-cc-pvtZ. It is likely that the theoretical $\Delta G°$ values are subject to large uncertainties because they depend on the level of theory, and because the thermal corrections are large and take no account of vibrational anharmonicity. The experimental values must also be regarded with caution due to the several assumptions contained in the structural model for the system.

Acknowledgment. The early work in this investigation was supported by the National Science Foundation. During its long history there has been useful interaction with many colleagues, of whom Grete Gundersen, Kolbjørn Hagen, and Alan Robiette deserve special thanks.

Supporting Information Available: Table of the symmetry coordinates and force field from theory (B3LYP/6-311+G(d)); table showing the internal coordinates with atom numbering on diagrams of the trans and cis conformers; table of wavenumbers of the normal modes with descriptions; table of the experimental molecular scattered intensity. This material is available free of charge via the Internet at http://pubs.acs.org.

References and Notes

(1) For simplicity the terms "cis" and "trans" are used throughout to designate the more accurate "syn periplanar" and "anti periplanar".
(2) Groth, P.; Hassel, O. *Acta Chem. Scand.* **1962**, *16*, 2311.
(3) Hencher, J. L.; King, G. W. *J. Mol. Spectrosc.* **1965**, *16*, 158.
(4) Kidd, K. G.; King, G. W. *J. Mol. Spectrosc.* **1968**, *28*, 411.
(5) Shimada, H.; Shimada, R.; Kanda, Y. *Bull. Chem. Soc. Jpn.* **1968**, *41*, 1289.
(6) Hencher, J. L.; King, G. W. *J. Mol. Spectrosc.* **1965**, *16*, 168.
(7) Durig, J. R.; Brown, S. C.; Hannum, S. *J. Chem. Phys.* **1971**, *54*, 4428.
(8) Durig, J. R.; Hannum, S.; Baglin, F. G. *J. Chem. Phys.* **1971**, *54*, 2367.
(9) Goubeau, J.; Adelhelm, M. *Spectrochim. Acta, Part A* **1972**, *28*, 2471.
(10) Sander, S.; Willner, H.; Khriachtchev, L.; Pettersson, M.; Rasanen, M.; Varette, E. L. *J. Mol. Spectrosc.* **2000**, *203*, 145.
(11) Hagen, K.; Hedberg, K. *J. Am. Chem. Soc.* **1973**, *95*, 1003.
(12) Hassett, D. M.; Hedberg, K.; Marsden, C. J. *J. Phys. Chem.* **1993**, *97*, 4670.
(13) Danielson, D. D.; Hedberg, L.; Hedberg, K.; Hagen, K.; Trætteberg, M. *J. Phys. Chem.* **1995**, *99*, 9374.
(14) Hagen, K.; Hedberg, K. *J. Am. Chem. Soc.* **1973**, *95*, 4796.
(15) Friesen, D. T., Ph.D. Thesis, Oregon State University, 1981.
(16) Marstokk, K.-M.; Møllendal, H. *Acta Chem. Scand.* **1995**, *49*, 172.
(17) Data reduction: Gundersen, G.; Hedberg, K. *J. Chem. Phys.* **1969**, *51*, 2500. (b) background removal: Hedberg, L. *Abstracts*; Fifth Austin Symposium on Gas-Phase Molecular Structure; University of Texas: Austin, TX, 1974; p 37.
(18) Ross, A. W.; Fink, M.; Hilderbrandt, R. L. *International Tables for Crystallography*; International Union of Crystallography; Kluwer: Boston, MA, Dordrecht, The Netherlands, and London, 1992; Vol. 4, p 245.
(19) Frisch, M. J.; Trucks, G. W.; Schlegel, H. B.; Scuseria, G. E.; Robb, M. A.; Cheeseman, J. R.; Montgomery, J. A., Jr.; Vreven, T.; Kudin, K. N.; Burant, J. C.; Millam, J. M.; Iyengar, S. S.; Tomasi, J.; Barone, V.; Mennucci, B.; Cossi, M.; Scalmani, G.; Rega, N.; Petersson, G. A.; Nakatsuji, H.; Hada, M.; Ehara, M.; Toyota, K.; Fukuda, R.; Hasegawa, J.; Ishida, M.; Nakajima, T.; Honda, Y.; Kitao, O.; Nakai, H.; Klene, M.; Li, X.; Knox, J. E.; Hratchian, H. P.; Cross, J. B.; Adamo, C.; Jaramillo, J.; Gomperts, R.; Stratmann, R. E.; Yazyev, O.; Austin, A. J.; Cammi, R.; Pomelli, C.; Ochterski, J. W.; Ayala, P. Y.; Morokuma, K.; Voth, G. A.; Salvador, P.; Dannenberg, J. J.; Zakrzewski, V. G.; Dapprich, S.; Daniels, A. D.; Strain, M. C.; Farkas, O.; Malick, D. K.; Rabuck, A. D.; Raghavachari, K.; Foresman, J. B.; Ortiz, J. V.; Cui, Q.; Baboul, A. G.; Clifford, S.; Cioslowski, J.; Stefanov, B. B.; Liu, G.; Liashenko, A.; Piskorz, P.; Komaromi, I.; Martin, R. L.; Fox, D. J.; Keith, T.; Al-Laham, M. A.; Peng, C. Y.; Nanayakkara, A.; Challacombe, M.; Gill, P. M. W. Johnson, B.; Chen, W.; Wong, M. W.; Gonzalez, C.; Pople, J. A. *Gaussian 03*, revision B.05; Gaussian, Inc.: Pittsburgh, PA, 2003.
(20) Hedberg, L.; Mills, I. M. *J. Mol. Spectrosc.***1993**, *160*, 117. Hedberg, L.; Mills, I. M. *J. Mol. Spectrosc.* **2000**, *203*, 82.
(21) Friesen (ref 14) tested the two other model types, but found that the third one based on the nonlocalized set of pseudoconformers was best.
(22) The choice of trans instead of cis for $\phi = 0°$ fits eq 1. This choice was convenient because D.T.F.'s thesis work used this definition. However, all results have been transformed to be consistent with $\phi = 180°$ for the trans form.
(23) Tsuchiya, S. *J. Mol. Struct.* **1974**, *22*, 77.
(24) Danielson, D.; Patton, J. V.; Hedberg, K. *J. Am. Chem. Soc.* **1977**, *99*, 6484.
(25) Ryan, R. R.; Hedberg, K. *J. Chem. Phys.* **1969**, *50*, 4986.
(26) Shen, Q.; Hedberg, K. *J. Phys. Chem. A* **1998**, *102*, 6470.
(27) Because the pseudoconformers around 100° receive relatively small Boltzmann weights, the exact values of the minima are unimportant.